

Document downloaded from:

<http://hdl.handle.net/10251/208382>

This paper must be cited as:

Rueda-García, L.; Tasquer-Val, D.; Calderón-Bofias, P.; Calderón García, PA. (2024). Detecting wire breaks in prestressed concrete pipes: an easy-to-install distributed fibre acoustic sensing approach. *Structural Health Monitoring*.
<https://doi.org/10.1177/14759217241236365>



The final publication is available at

<https://doi.org/10.1177/14759217241236365>

Copyright SAGE Publications

Additional Information

1 **Detecting Wire Breaks in Prestressed Concrete Pipes: An Easy-to-** 2 **Install Distributed Fibre Acoustic Sensing Approach**

3 Lisbel Rueda-García,¹ Daniel Tasquer-Val,¹ Pedro Calderón-Bofías² and Pedro A. Calderón³

4 ¹ Concrete Science and Technology University Institute (ICITECH), Universitat Politècnica de
5 València (UPV), Valencia 46022, Spain.

6 ² CalSens S.L., Valencia 46022, Spain.

7 ³ Department of Construction Engineering and Civil Engineering Projects, Concrete Science
8 and Technology University Institute (ICITECH), Universitat Politècnica de València (UPV),
9 Valencia 46022, Spain.

10 Correspondence should be addressed to Lisbel Rueda-García; lisruega@upv.es

11 **Abstract**

12 The escalating water stress resulting from drought conditions in certain global regions
13 underscores the imperative to minimize water losses, particularly within drinking water supply
14 networks. One way to achieve this is by improving pipe monitoring systems to allow the early
15 detection of possible structural collapse of the pipes. One type of pipe widely used in water
16 mains is the prestressed concrete pipe, whose main cause of structural failure is the breakage
17 of prestressing wires. This research paper analyses the ability of an easy-to-install DAS
18 (Distributed Acoustic Sensing) monitoring system using fibre optics to identify and locate the
19 acoustic signal produced by the wire breaks in prestressed concrete pipes to make early
20 detection of possible structural failures. For this purpose, a large experimental pipeline stretch
21 was built (approximately 1 m in diameter and 40 m long) where wire breaks were simulated.
22 Several variables were studied: the origin of the signal (to distinguish wire breaks from events
23 of a similar nature), the location of the event in the pipe, the presence of background noise, the
24 internal water pressure, the length of the prestressed wire not subject to bonding with the
25 concrete and the presence of water in the pipe. The results showed that the DAS system could
26 detect almost all events. In addition, two of the multiple parameters measured in the signals,
27 the zero-crossing rate and the short-time energy, made it possible to precisely determine the
28 signal's origin and the event's location. Another parameter measured, the duration of the signal
29 in this case, made it possible to differentiate whether the events had occurred when the pipe
30 was empty or full of water. These and other results in this paper present a highly promising
31 perspective on using this DAS system in water main monitoring.

32 **Keywords:** distributed acoustic sensing, fibre optic, prestressed concrete pipe, water main,
33 wire break, structural failure, monitoring

34 **1. Introduction**

35 As indicated in the Technical report of the European Commission, “Drought in Europe March
36 2023”¹, much of Europe is currently under severe water stress due to an exceptionally dry and
37 warm winter. Water scarcity is forcing a rethink of how the exploitation and supply of drinking
38 water have historically been managed. To efficiently manage natural resources during the
39 supply process, minimising losses in drinking water supply systems is necessary. One of the

40 events that cause significant water losses is the structural failure of pipes in water supply
41 networks. One way to avoid these losses is to detect early and precisely where these structural
42 failures will occur so that it is possible to repair or replace these pipes before the failure occurs.

43 Since the mid-last century, many water operators have used prestressed concrete pipes in their
44 pipelines because they provide durable, cost-effective solutions for large-diameter mains ². For
45 example, in the USA and Canada alone, more than 30,000 km of this type of pipe were reported
46 in major water utilities in 2000 ³, with many of the lines currently in use being more than 50
47 years old. Although the performance of this type of pipe has traditionally been very reliable,
48 one of the problems that most affect prestressed concrete pipes, and their main cause of failure,
49 is the breakage of the prestressing wires, also known as “wire breaks” ⁴⁻⁶. Wire breaks can have
50 different causes, such as corrosion, hydrogen embrittlement, high internal pressures, or
51 overloading ⁷, with corrosion being the main cause ⁶. Wire breaks cause the concrete core to
52 deconfine. Thus, when a threshold number of broken wires is exceeded, the pipe fails at a load
53 below its design strength. Corroded precast concrete pipes are prone to explosive failure during
54 rapid changes in pipeline operation, such as periods of high demand, fire suppression, and heat
55 waves ⁴. The structural collapse of precast concrete pipes costs significant sums of money due
56 to the repair or replacement of the pipes and the effect on other existing infrastructures where
57 the pipes are buried. It could also present a public health problem due to possible contamination
58 of the drinking water supply.

59 For all these reasons, it is very important to monitor the water mains to detect broken wires and
60 to be able to act before reaching the structural failure of the pipes. In existing prestressed
61 concrete pipes, the main inspection techniques used to know the current state of the pipe in
62 terms of number of broken wires are (i) internal visual and sound inspections, where qualified
63 personnel walk inside the pipe to perform a visual inspection and impact the interior surface to
64 identify hollow sounds typical of delaminated areas in the pipe, and (ii) electromagnetic
65 inspections, where electromagnetic equipment, which detects the continuity of the prestressing
66 steel and estimates the number of broken strands, is pushed inside the empty pipes ². In new or
67 inspected pipelines, acoustic monitoring is sometimes carried out by continuously monitoring
68 the acoustic activity of the pipeline to identify the acoustic event associated with a wire break.
69 This has traditionally been done using hydrophone arrays ⁸. This technique, in which
70 hydrophones are attached to hydrants or other network elements, has been widely used due to
71 its effectiveness in water mains. However, they have certain limitations, such as the difficulty
72 of using them in deep buried pipes and the signal attenuation with distance from the
73 hydrophone. In the last 20 years, another acoustic monitoring system has been developed using
74 fibre optic sensors ^{2,9}, known as distributed acoustic sensing (DAS). The system allows the
75 monitoring of several kilometres of pipes with a single data acquisition device. With this
76 system, the attenuation of signals from an acoustic event is minimal. In addition, many of the
77 traditional monitoring techniques require the dewatering of the pipelines and entail the risk of
78 entering confined spaces. This is why the current trend is towards developing monitoring
79 systems that allow their implementation without draining the pipe, that can be placed in both
80 exposed and deep buried pipes, and that do not require the entry of large equipment or people
81 inside them.

82 DAS is a fibre optic sensing technology that has rapidly developed in recent years, which
83 allows continuous and real-time monitoring of physical phenomena such as acoustic vibrations,
84 temperature changes, and strain. The technology works by sending pulses of light through an
85 optical fibre cable and then measuring the changes in the backscattered light caused by external

86 disturbances or vibrations. Since the entire fibre cable acts as a sensor, the cable is never further
87 than a pipe diameter from a wire break ⁹. DAS has multiple advantages, such as anti-
88 electromagnetic interference, corrosion resistance, slenderness, and flexibility ¹⁰. In addition,
89 installing a fibre optic cable with various cores can be used for other purposes, such as
90 telecommunication transmission. The application of this technology to linear infrastructure
91 monitoring has broad potential. However, it faces many challenges, such as the vast amounts
92 of monitoring data, the directional sensitivity of fibre optic cables, the longitudinal positioning
93 of the fibre optic cables along the pipeline and the difficulties in processing data ¹⁰, as well as
94 the placement of the cable in the pipeline through a simple and effective installation for locating
95 wire breaks.

96 Recent research on using DAS technology in pipeline monitoring involves different types of
97 fibre optic cable installation. For example, many researchers directly paste cables onto pipe
98 walls, either along the pipe ¹¹ or even helically around the pipe ¹²⁻¹⁵. Although this surface-
99 glued cable method may be more effective, it requires digging up the pipe for sensing or even
100 going inside it, as in ¹⁶, which is very expensive and impractical. As explained in ¹⁰, other
101 researchers bury cables in the ground soil near pipelines, as in ¹⁷⁻¹⁹. Others place the fibre optic
102 cable outside an uncovered pipe, at some distance from it ²⁰, which would be less practical in
103 a real application because of the danger of fibre interactions with external agents due to being
104 exposed. Another group of authors ^{2,9,21-23} started in 2005 to introduce the fibre optic cable
105 inside the pipe without gluing it to the inner wall. In particular, Higgins and Paulson in ² showed
106 an installation of the cable by pushing the fibre optic coil with a trolley along the inside of the
107 waterless pipe and attaching the fibre to strain relief devices in the form of a metal ring attached
108 to the inner wall of the pipeline. This type of installation was used in other real applications by
109 the same group ²¹⁻²³. Other professionals in this group indicated in ⁹ that in the monitoring
110 project of a section of the Great Man-Made River pipeline (Libya), which is one of the most
111 significant water projects in the world, for the first time, it was intended to install the fibre optic
112 cable using a parachute to pull the cable into place while the pipeline was in operation, without
113 the need of dewatering the pipeline as had been done in previous projects. This type of
114 installation would be the simplest and cheapest, although it carries the risk of poorer signal
115 detection due to the attenuation caused by the medium surrounding the cable.

116 This paper studies the ability of an easy-to-install DAS system, in which the fibre optic cable
117 is laid inside the pipeline without the need for internal fixings and with the possibility of being
118 installed while the pipeline is in operation, to identify and locate the acoustic signal produced
119 by the breakage of wires in prestressed concrete pipes to carry out early detection of possible
120 structural failures. For this purpose, an extensive test programme was carried out in which the
121 DAS system was installed in a large experimental pipeline stretch. In the tests, wire breaks
122 were simulated by opening windows in the mortar of the prestressed pipes to gain access to the
123 wires and cutting them with a shear. Through this experimental programme, multiple variables
124 are studied in this article to analyse the capacity of the DAS to detect wire breaks in different
125 situations accurately. These variables are (i) the origin of the signal, through the study of the
126 ability of the DAS system to differentiate wire breaks from other signals of a similar nature,
127 such as those generated by hitting the pipe with a hammer and noises caused by unidentified
128 events; (ii) the location of the signal origin; (iii) the presence of background noise; (iv) the
129 internal water pressure in the pipeline; (v) the size of the window in which the wire cut is
130 executed; and (vi) the presence or not of water in the pipe.

131 The present research work provides valuable data obtained under controlled conditions from
132 one of the largest experimental pipelines in the literature purposely created for this research,
133 which increases the state of knowledge on the subject. In addition, multiple variables that can
134 occur in real conditions are studied. Additionally, the research presents an easy-to-install
135 system, as it uses a robust fibre optic cable, which is very easy to handle, and therefore does
136 not require installation by qualified personnel. The contribution of this research in relation to
137 the signal processing carried out is also interesting. Consequently, the present study supports
138 the development of DAS as a continuous, remote, highly sensitive, resistant, simple, and
139 passive monitoring system, making it attractive for real applications in pipeline monitoring.

140 **2. Materials and Methods**

141 **2.1. Test variables**

142 To achieve the objectives of this research, a test programme was designed to simulate and
143 detect wire breaks. For this purpose, an experimental pipeline of almost 40 m in length, which
144 included two prestressed concrete pipes, was built, into which the fibre optic cable of the DAS
145 system used was introduced (the details of this test programme are given in the following
146 sections). The experimental programme included the study variables described in the following
147 paragraphs.

148 Origin of the acoustic signal. The main signal origin studied was the breakage of the prestressed
149 concrete pipe steel wires. In addition, the signals originating from the hitting of the pipes with
150 a hammer were analysed to observe the differences with wire break signals, as hammer blows
151 produce sudden signals and therefore have certain similarities with wire break signals.
152 Unidentified event signals were also analysed to differentiate them from the previous two. The
153 unidentified events were events observed in the signal recorded by the DAS system that had
154 similar characteristics to wire breaks but did not come from any event performed on purpose
155 in the pipeline, so their origin is unknown.

156 Location of the signal origin. The wire breaks and the hammer blows were performed at various
157 points of the experimental pipeline to analyse the ability of the DAS system to provide the
158 location of the signal origin.

159 Presence of background noise. To identify wire breaks when there are also continuous acoustic
160 signals from devices or machines, the various acoustic events (wire breaks, hammer blows and
161 unidentified events) were also analysed in the presence of noise from a portable power
162 generator placed on a buried section of the pipeline.

163 Internal water pressure in the pipeline. Given the limitations of the experimental setup, the tests
164 with the pipe full of water were carried out without water flow. However, the water pressure
165 could be varied, so signals were produced at different water pressures to detect variations in
166 the signal captured by the DAS system according to the internal water pressure in the pipe.
167 These pressures were 0, 0.5, 1.0, 2.0, 3.0, 4.0 and 5.0 bar.

168 Size of the window in the concrete. Corrosion of prestressing wires often causes spalling of the
169 mortar above the wires, usually before the wire breaks. To detect differences in the signal
170 generated by wire breaks depending on the length of the uncovered wire, windows of different

171 sizes were opened in the mortar coating and different wire breaks were caused in them.
 172 Specifically, four window sizes were used: 8, 15, 30 and 60 cm.

173 Presence of water in the pipeline. To study the ability of the DAS system to recognise signals
 174 in different media, signals were generated with the pipeline full of water and empty.

175 Considering all the variables described above, the present experimental programme seeks to
 176 analyse the signal produced by the 138 events shown in Table 1.

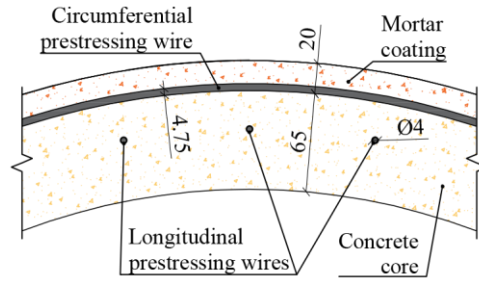
177 Table 1: Summary of events analysed in the experimental programme.

Event type	Height of the window in the mortar [cm]	Without water	With water	TOTAL
Wire breaks	8	2	3	5
	20	7	16	23
	30	1	3	4
	60	3	3	6
Wire breaks + power generator	20	0	8	8
Hammer blows	-	7	47	54
Hammer blows + power generator	-	0	4	4
Unidentified events	-	15	15	30
Unidentified events + power generator	-	0	4	4
TOTAL	-	35	103	138

178 **2.2. Prestressed concrete pipes**

179 There are different types of prestressed concrete pipes depending on their layering. They all
 180 have a concrete core and a prestressing wire covered by a mortar coating. In addition, the pipes
 181 can have a steel cylinder (prestressed concrete cylinder pipes, PCCP), which can be embedded
 182 in the concrete core (embedded-cylinder pipes, ECP) or line the concrete core, so the
 183 prestressing wire is wrapped directly on the steel cylinder (lined cylinder pipe, LCP). If no steel
 184 cylinder exists, the prestressing wire is wrapped directly on the concrete core (prestressed
 185 concrete non-cylinder pipe, PCNP). In these tests, two PCNPs were used. The two pipes were
 186 removed from a drinking water pipeline installed in 1969, which was in operation until
 187 recently. The design pressure was 7.5 bar, and the operating pressure was 6.5 bar. The pipes
 188 were in perfect condition after removal.

189 The PCNPs tested had a length of 4 m, an outer diameter of 1020 mm and an inner diameter of
 190 850 mm. The tubes had the layers shown in Figure 1. The circumferential prestressing wire
 191 had a diameter of 4.75 mm and a spacing of wire of 28.75 mm. The concrete core had
 192 longitudinal prestressing wires of 4.00 mm diameter every 83 mm (35 wires).



193

194

Figure 1: Layering diagram of the PCNPs tested (units: mm).

195

196

197

198

199

200

201

202

203

204

Due to the age of the pipes, their mechanical properties at manufacture are unknown. However, characterisation tests were carried out to obtain the present mechanical properties relevant to this study. These are the tensile strength and modulus of elasticity of the circumferential prestressing wire and the prestressing stress of the wire. To obtain the former, a tensile test was carried out according to UNE-EN ISO 6892²⁴ by averaging the results of three tests. The resulting tensile strength of the prestressing wire was 1,656 MPa, and its modulus of elasticity was 159,250 MPa. To obtain the prestressing stress, a window was made in the mortar coating to access the wire, and a strain gauge was placed on the wire. The wire exposed in the window was cut while the pipe was empty to obtain the strain recovered by the wire after cutting. From the modulus of elasticity and the strain, a prestressing stress of 712 MPa was obtained.

205

2.3. Experimental setup

206

207

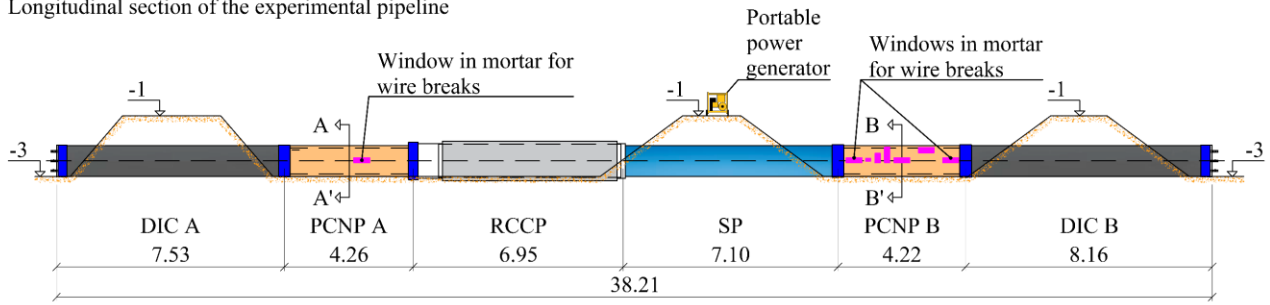
208

209

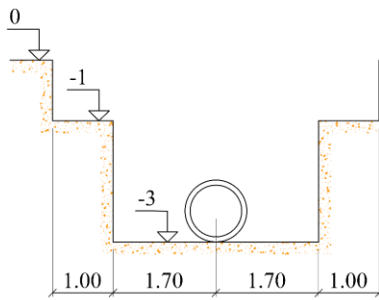
210

A 38 m-long experimental pipeline was built for field tests. The pipeline length was chosen to be long enough to have inside at least three 10-meter segments of fibre optic since, as explained in Section 2.4, the spatial resolution of the DAS system used was 10 m. To accommodate the pipeline, a trench that was 3 m deep and had a 1-meter high berm and 3.4-meter wide base was excavated, as illustrated in Figure 2.

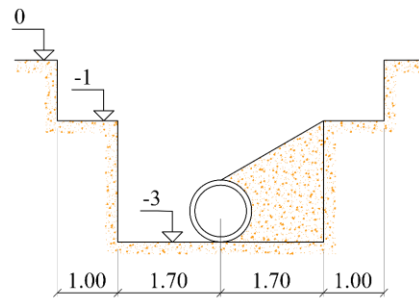
Longitudinal section of the experimental pipeline



Cross-section A-A'



Cross-section B-B'



Diameter of pipes

Pipe	\varnothing_{ext} (mm)	\varnothing_{int} (mm)
PCNP	1020	850
RCCP	1300	1100
DIC	1048	1000
SP	1018	1000

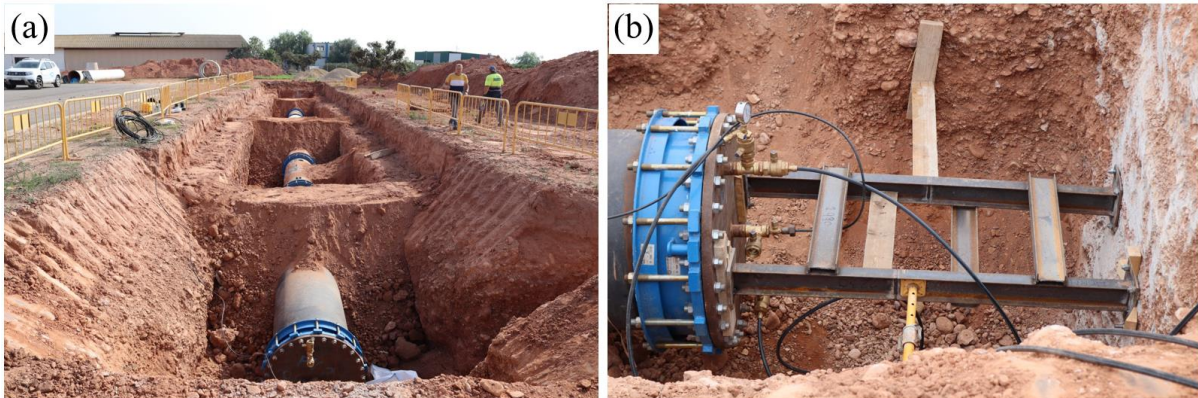
211

212

Figure 2: Experimental pipeline dimensions (units: m).

213 The experimental pipeline was built using two prestressed concrete non-cylinder pipes (PCNP
 214 A and PCNP B), one reinforced concrete cylinder pipe (RCCP), two ductile iron pipes (DIC A
 215 and DIC B) and one steel pipe (SP) ranging from 1018 to 1300 mm outer diameter, as shown
 216 in Figure 2. The two PCNPs, the subject of this study, were spaced approx. 14 m apart to have
 217 sufficiently separated signal locations. Furthermore, the PCNPs were sufficiently separated
 218 from the start and end of the pipeline by providing additional pipes (the two DICs) to ensure
 219 that the 10-meter segments of fibre optic that capture the signals produced in the PCNPs are
 220 entirely within the pipeline. The two ends of the piping were closed by blind flanges with
 221 different valves to introduce the fibre optic cable and to fill the piping with water. A manometer
 222 was installed in one of these valves to control the internal water pressure. The tests were carried
 223 out without water flow.

224 Although certain pipeline stretches had to be left uncovered to perform the tests and access the
 225 pipe couplings for adjustment during the tests, as much of the pipeline as possible was buried
 226 to simulate real conditions (see Figure 2 and Figure 3a). A concrete wall approx. 0.5-metre
 227 thick was placed at each end of the excavation to secure the shoring of the blind flanges (Figure
 228 3b). Lateral shoring was also provided at the pipe couplings to prevent lateral displacement of
 229 the unburied pipes due to the rise in internal water pressure. The portable power generator to
 230 introduce background noise during some tests was placed on the buried section of the SP (see
 231 Figure 2).



232

233 Figure 3: Photographs of the test area. (a) Overview of the experimental pipeline. (b) One of the blind flanges.

234 **2.4. Wire breaks**

235 To make the different cuts in the prestressing wires of the PCNPs, windows of various sizes
 236 were opened in the mortar coating with the help of a radial saw and a hammer drill (see Figure
 237 4a), with a procedure similar to that used by other authors^{7,21}. In the first PCNP (PCNP A in
 238 Figure 2), a 15 cm high window was made. In the second PCNP (PCNP B in Figure 2), one 8
 239 cm high window, four 15 cm high windows, one 30 cm high window and one 60 cm high
 240 window were opened.



241

242 Figure 4: Preparation of prestressed concrete pipes. (a) Example of opening a 15 cm high window in one of the
 243 prestressed concrete pipes. (b) Wire break with a shear.

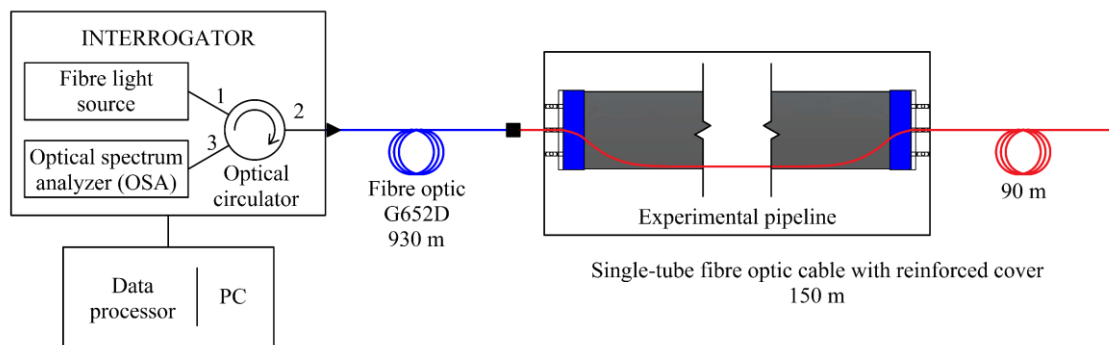
244 Wire breaks in PCNPs were simulated by cutting with a shear (see Figure 4b), as other authors
 245 did²². This method was chosen for its simplicity, speed and for reducing the extra noise during
 246 cutting compared to other tools, such as the radial saw. The aim was to simulate as closely as
 247 possible the wire break that would occur in an actual situation due to corrosion of the
 248 reinforcement. Furthermore, the suitability of this method was confirmed by the publication of
 249 Li et al.¹⁵, where the wires were artificially broken with a radial saw and electrochemical
 250 corrosion, and it was found that the signal generated by the corrosion was almost identical to
 251 that caused by the artificial breakage of the bar.

252 **2.5. Distributed acoustic sensing system**

253 The monitoring system used in this research was a type of distributed acoustic sensing (DAS).
254 The DAS technology employed is based on Chirped-pulse Φ -OTDR (Phase-Sensitive Optical
255 Time-Domain Reflectometry), a variant of the classic Φ -OTDR. Φ -OTDR systems can detect
256 disturbances in the fibre by recovering the induced phase information from the backscattered
257 light travelling through the fibre core. The vibration's location and intensity can be obtained in
258 this way. Chirped-pulse Φ -OTDR uses linearly chirped pulses to measure distributed strain and
259 temperature changes in a single shot without requiring a frequency scan²⁵. As explained by
260 Pastor Graells in²⁵, the system's complexity is not noticeably higher than classic Φ -OTDR
261 while it maintains the best aspects of that method: fast measurements are possible with a
262 bandwidth only constrained by the length of the fibre (potentially across several tens of
263 kilometres with metric spatial resolutions), and temperature/strain fluctuations are measured
264 with resolutions several orders of magnitude lower than Brillouin.

265 The DAS system used in this research had one nano-strain sensitivity, 10-metre spatial
266 resolution, 90-kilometre maximum range, high low-frequency performance, high signal-to-
267 noise ratio²⁶ and no fading. The fibre optic cable used was a single-tube cable with a reinforced
268 cover and loose single-mode fibres. This type of cable was selected following satisfactory
269 results in previous studies by the research group. The cable has the advantages of being robust,
270 watertight and inert in interaction with water, making it very suitable for insertion inside
271 drinking water pipes without requiring highly specialised personnel or instrumentation due to
272 its high resistance. Furthermore, only one of the fibres is used in the DAS so that the rest can
273 be used for other purposes, such as telecommunications transmission.

274 The setup diagram is shown in Figure 5. A 930-metre fibre optic coil that acts as a reference
275 was fused between the measuring cable and the interrogator. This coil was a single-mode
276 optical fibre cable. The coil was introduced in a box to insulate it from outside noise. After the
277 experimental stretch, 90 m of the measuring cable was left over. The fibre optic cable was
278 introduced in the experimental pipeline while it was empty through one of the ends before
279 closing it with the blind flange. The cable was laid down on the inner base of the pipeline with
280 no tension.



281

282

Figure 5: Setup diagram of the DAS system installed for the tests.

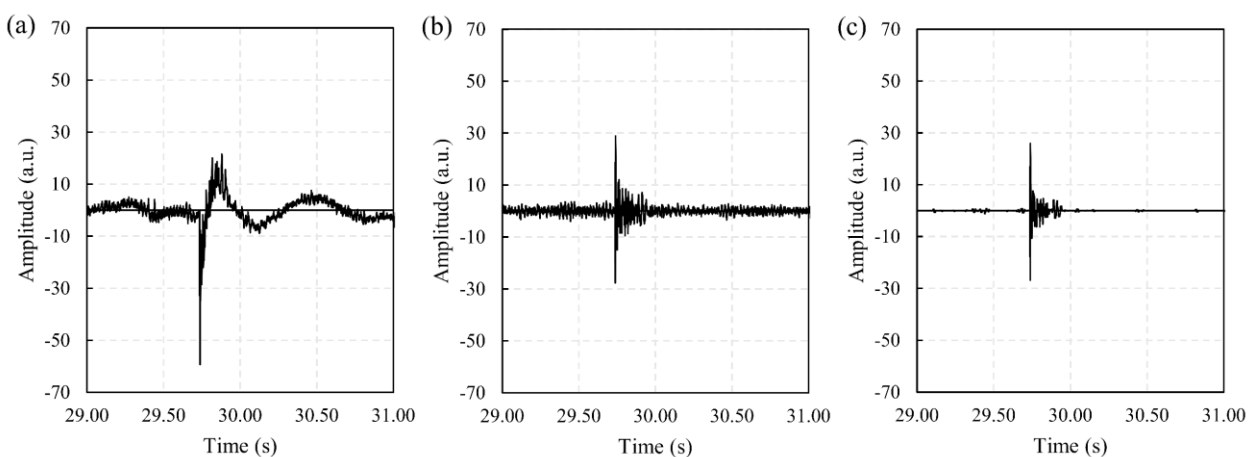
283 2.6. Test procedure

284 The tests were carried out in four different days. The sampling frequency of the DAS system
285 was set at 1 kHz. In all the tests, hammer blows were dealt at the beginning and end of the
286 pipeline to determine the fibre optic cable segment inside the pipe. For each wire break and
287 hammer blow, the location of the event, the internal water pressure and the time of execution
288 of the event were recorded for searching the events in the files generated by the DAS system.
289 A total of 104 events were performed, 46 of which were wire breaks and 58 were hammer
290 blows (see Table 1). In addition, 34 unidentified events were analysed.

291 3. Results and Discussion

292 3.1. Pre-processing of the original signal

293 When no tests were being run on the pipeline, i.e., during the idle situation, it was observed
294 that the environmental and system noise had low frequencies with very high amplitude, much
295 higher than that corresponding to the higher frequencies of interest in these tests. Consequently,
296 a high-pass filter with a cutoff frequency of 30 Hz was employed to facilitate the visualisation
297 of the data. The result of using this filter can be seen in the example in Figure 6a-b. In addition,
298 other denoising filters were applied to clean the signal from the existing ambient noise to
299 improve the detection of the programmed events. A discrete wavelet analysis (DWT) was
300 carried out. The Haar wavelet transform was used with four levels, as in ¹⁵. The efficiency and
301 simple calculation of this filter allow the results to be processed in real-time, which is very
302 important for the application of the system as continuous monitoring. In addition, the Minimax
303 denoising methodology, also used in ¹⁵, is used as a thresholding rule since it is beneficial for
304 signals with complex structures and important features that need to be preserved during
305 denoising. The soft threshold function is also applied for better continuity of the signal. All this
306 results in an amplitude-time plot that makes recognising the signals produced during the test
307 easier. Figure 6b-c shows an example of the signal produced by a wire break in a cable segment
308 inside the pipeline with and without the denoising filter.



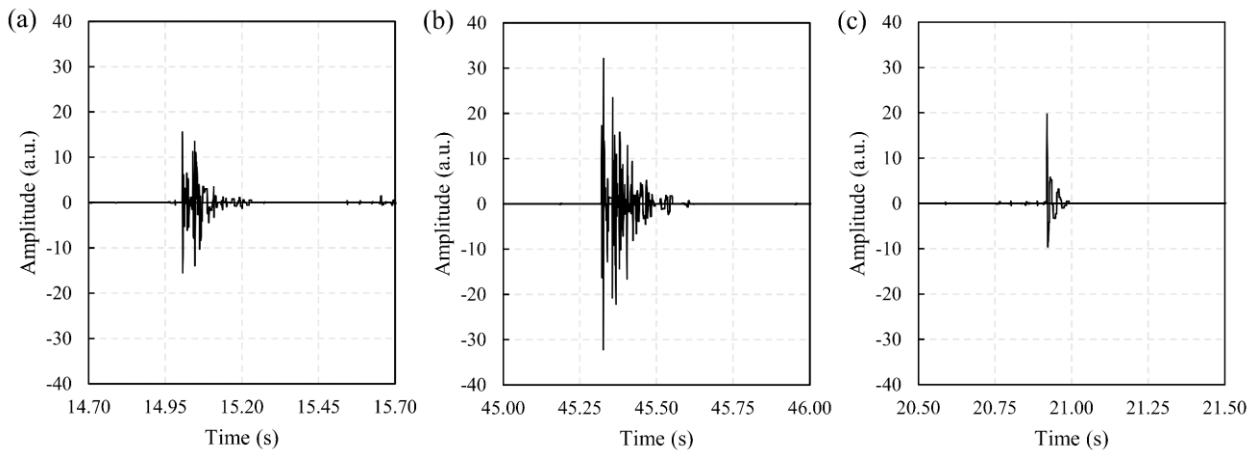
309

310 Figure 6: Example of the signal during a wire break. (a) Without filters. (b) With a high-pass filter. (c) With a
311 high-pass filter and denoising filter.

312 The filters used proved to be appropriate to remove a significant part of the ambient and system
313 noise from the signal without impairing the recognition of the test signals (wire breaks and
314 hammer blows) and to show more clearly where the signals are located.

315 3.2. Detection of the events and signal parameters used for the analysis

316 Clean signals were obtained after applying the relevant filters to the signal, as in the examples
317 in Figure 7. This figure shows representative examples of the signal produced by a wire break
318 (Figure 7a) and by hitting a pipe with a hammer (Figure 7b). As can be seen, both signals have
319 similar characteristics: they show a sudden large amplitude that attenuates over time. On the
320 other hand, the signals produced by unidentified events all showed similar characteristics to
321 the example in Figure 7c. Because of their similarity to the signals produced by wire breaks,
322 these were also studied in this article to find the parameters that differentiate them from the
323 other signals.



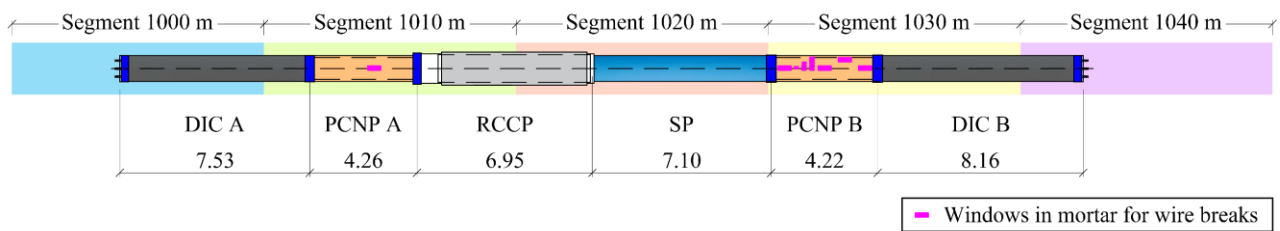
324

325 Figure 7: Examples of signals obtained from each type of event analysed in this paper. (a) Wire break. (b)
326 Hammer blow. (c) Unidentified event.

327 Due to the characteristics of the signals studied in this article, the following five signal
328 parameters were obtained for each event: (i) maximum absolute amplitude (in a.u.); (ii) zero-
329 crossing rate (ZCR). This is the number of times the signal crosses the zero amplitude value in
330 a window of a given duration. Using a threshold of 1 a.u in these tests instead of zero was
331 considered appropriate to avoid possible low amplitude noise. A window of sufficient duration
332 to cover the entire signal was used; (iii) short-time energy (STE) (in a.u.²). This is the
333 accumulated energy under the signal curve for a given time window. A window of sufficient
334 duration to cover the entire signal was used; (iv) duration (in s). It is the duration of the signal
335 between its onset and complete attenuation; (v) dominant frequency (in Hz). It is the frequency,
336 between 30 and 500 Hz, that shows the highest amplitude. The first four parameters were
337 already used by Li et al. in ¹⁵ to analyse the signals produced by the wire breaks they studied
338 in their research. They proved to be good indicators of the characteristics of this type of signal.

339 The analysis procedure consisted of creating a database of all the events analysed (46 wire cuts,
340 58 hammer blows and 34 unidentified events). The described parameters were obtained from
341 their signals to compare them with each other and analyse the differences that characterise
342 them. Since the system's spatial resolution is 10 m, the data were collected in 10-meter fibre
343 segments. A graphical representation of the location of those 10-meter fibre segments along

344 the experimental pipeline is shown in Figure 8 for better understanding. All the parameters
 345 described above were obtained in three fibre segments in the case of wire breaks and hammer
 346 blows: the one in which the event originated, the one that showed the earliest onset of the signal
 347 produced by the event and the one that showed the highest value of ZCRxSTE. Regarding the
 348 unidentified events, as they are events observed in the signal itself during the analysis phase,
 349 their actual segment of origin is unknown, so the parameters obtained were always those
 350 corresponding to the segment with the highest ZCRxSTE. In all cases, this segment matched
 351 the segment with the earliest onset of the signal produced by the event, as unidentified events
 352 were generally only detected in one fibre segment, with no alteration of the signal being
 353 observed in the remaining segments.



354

355 Figure 8: Location and identification of the 10-meter fibre segments located in the experimental pipeline.

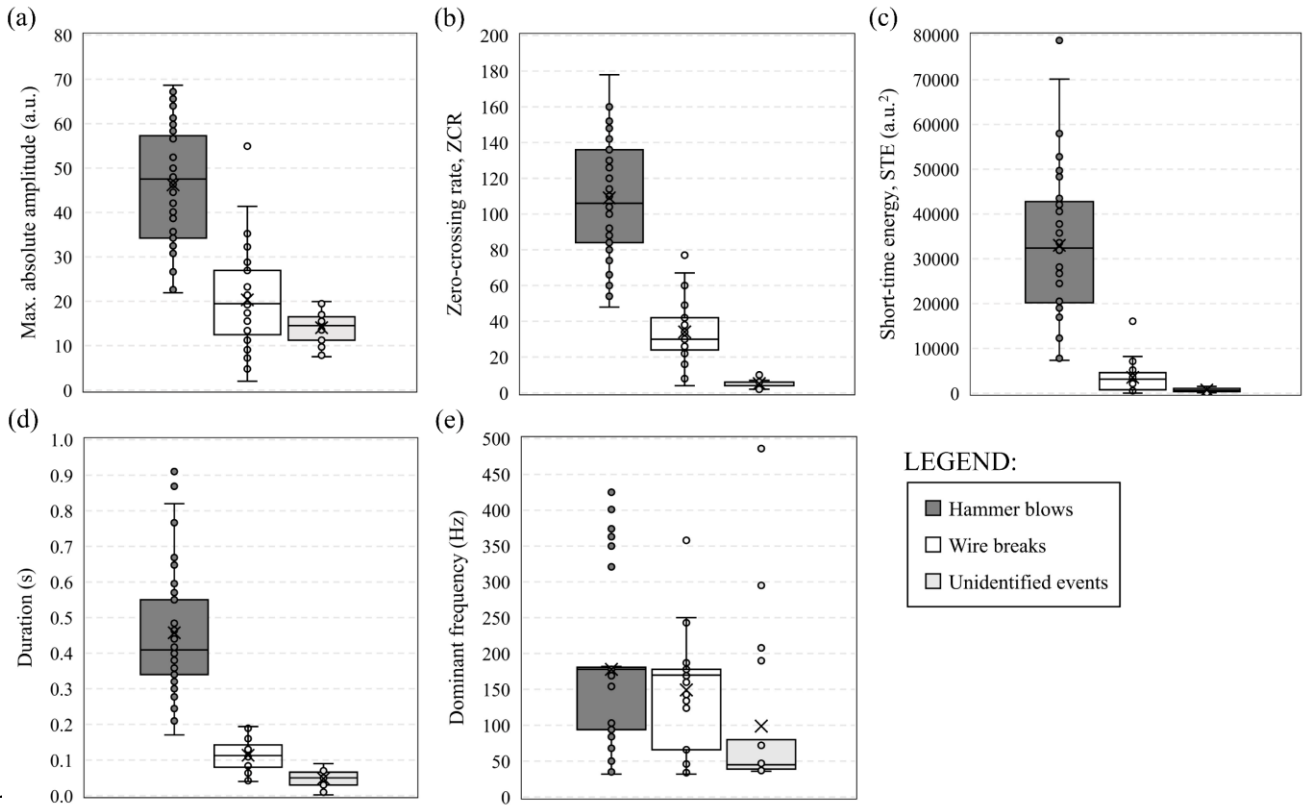
356 Of all the events performed in these tests, only three events, which were three of the five wire
 357 breaks performed in 8 cm high windows, were not detected in the signal measured by the DAS
 358 system through any of the parameters used in the analysis.

359 3.3. Effect of the test variables

360 3.3.1. Origin of the acoustic signal

361 One of the most relevant objectives of this research is to determine whether the monitoring
 362 system used can differentiate what caused the detected signal. For this reason, similar signals
 363 were studied to observe the system's capacity to distinguish them through the signal parameters
 364 analysed. These signals were those caused by hammer blows on the pipe walls, wire breaks in
 365 the PCNPs and noises detected during the tests.

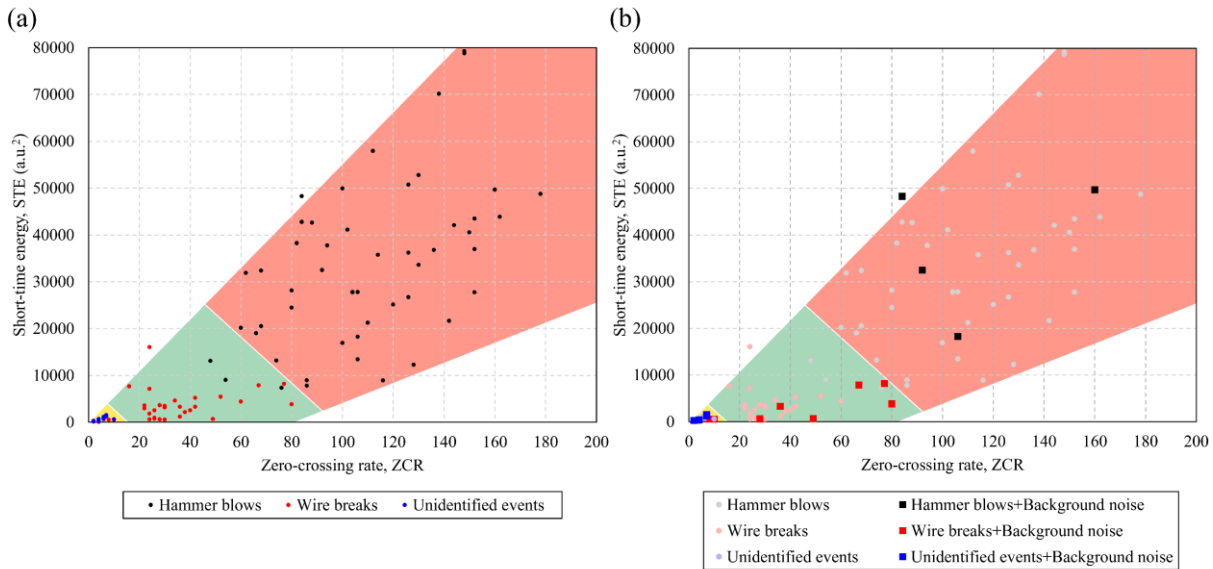
366 To determine which of the signal parameters analysed show differences depending on the
 367 signal's origin, the box-whisker plots in Figure 9 were produced. They represent each event's
 368 five signal indicators discussed in the previous section. These plots include all the events that
 369 took place in the pipeline with water, i.e., the events in the empty pipeline are excluded, as this
 370 is a different problem analysed later. Only the results from the 10-meter fibre segment with the
 371 highest ZCRxSTE are included in these graphs for the reasons explained later in Section 3.3.2.



373 Figure 9: Box-whisker plots of signals produced by hammer blows, wire breaks and unidentified events in the
 374 pipeline with water for the five parameters analysed. (a) Maximum absolute amplitude. (b) ZCR. (c) STE. (d)
 375 Duration. (e) Dominant frequency.

376 The box-whisker plots help us to observe the ranges in which the values of each parameter are
 377 found. It can be seen that both the ZCR and the STE show very different ranges for the three
 378 events analysed, which will allow us to find out the type of event that occurred. The duration
 379 of the signal also shows differences between the events, although the difference between the
 380 duration of a signal produced by a wire break and that produced by an unidentified event is not
 381 clear. As for the maximum absolute amplitude, no significant difference is observed between
 382 wire breaks and unidentified events. Concerning the dominant frequency, there are no
 383 differentiated ranges, which seems to indicate that the dominant frequency is not a parameter
 384 through which we can determine the origin of the signal when it comes to events such as those
 385 analysed in this paper since they are impulses that excite multiple frequencies at the same time
 386 without one predominating in the short time that the signal lasts.

387 In addition to analysing each indicator separately, each event was analysed through pairs of
 388 values. Thus, the same events were represented in a plot that relates the STE to the ZCR of
 389 each event (Figure 10a), and it was observed that the relationship between the ZCR and the
 390 STE differentiates quite clearly the type of event that occurred among the three analysed in this
 391 paper. In addition, the plotted point cloud shows three distinct areas to distinguish between
 392 events, as depicted in Figure 10a. Next to Figure 10a, Figure 10b is shown for ease of
 393 comparison. Its content will be explained in Section 3.3.3 below.



394

395
396
397

Figure 10: STE-ZCR plot of signals produced by hammer blows, wire breaks and unidentified events in the pipes with water. (a) All the events. (b) All the events, differentiating those with background noise and those without background noise (see Section 3.3.3).

398
399
400
401
402
403

The analysis shows that the DAS system used captured differences that allow the three event types studied to be identified quite accurately by defining ranges (upper and lower limits) for specific parameters. According to this study, the most revealing parameters were the ZCR and the STE. The identification of the event is improved by combining the results of both indicators, as shown in Figure 10a. This allows us to define a map in which the wire break phenomena are located in a clearly defined area that distinguishes them from other events.

404 3.3.2. Event location

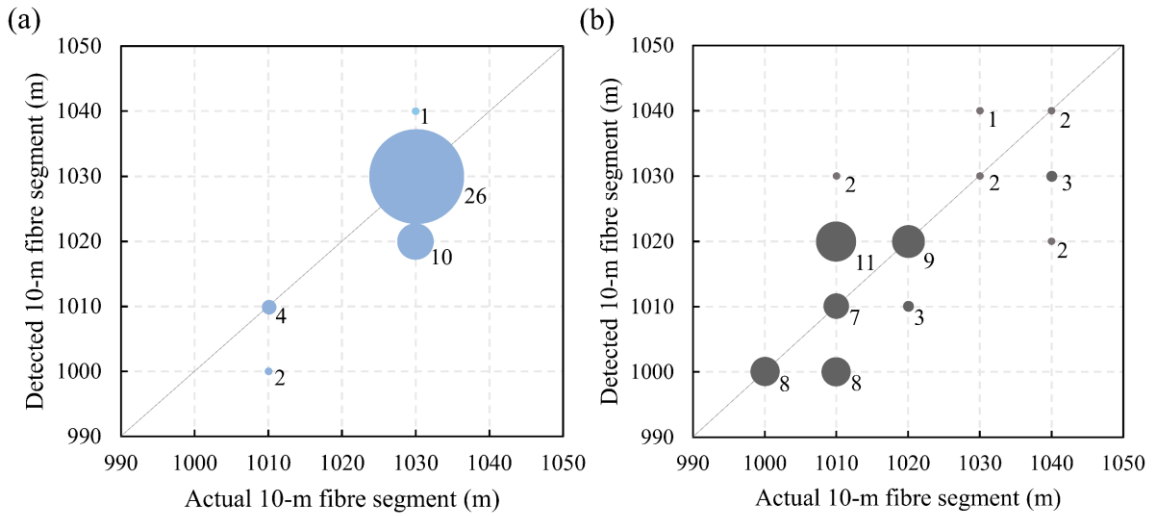
405
406
407
408
409
410
411
412
413
414
415
416

To determine the accuracy of the DAS system in locating events along the fibre, we obtained the percentage of events in which the 10-meter fibre segment showing the earliest signal onset coincided with the 10-meter fibre segment in which the signal originated. We also obtained the percentage of events where the 10-meter fibre segment with the maximum ZCRxSTE coincided with the 10-meter fibre segment where the signal originated. Both percentages were practically identical for both hammer blows and wire breaks. However, the authors have considered using the ZCRxSTE in all the analyses in this paper since both parameters are much easier to identify in an actual application with the DAS system studied than the onset in time of the acoustic signal. It should be noted that it was decided to use these parameters and not those of the stretch in which the signal originated since, in the implementation of an event detection algorithm, the origin of the events is unknown, so other criteria based on the parameters analysed must be used to study the effect on the signal of the different variables.

417
418
419
420
421
422
423

Figure 11 shows the relationship for both wire breaks and hammer blows between the actual location of the events, discretised into 10-meter fibre segments, and the location detected by the DAS, which is the one corresponding to the 10-meter fibre segment with the maximum ZCRxSTE of the signal. For a better understanding, see Figure 8 for the location and identification of the different segments. The results in Figure 11 are presented as a scatter plot, indicating the event density of each dot on the plot by the diameter of the dot and the number of events. Note that, while hammer blows were performed at multiple distances from the origin

424 of the pipe, wire breaks were only performed at the windows in the mortar coating located in
 425 Segments 1010 and 1030 m.



426

427 Figure 11: Relationship between the 10-meter fibre segment where the event is actually located and the 10-
 428 meter fibre segment where the event was detected by the DAS system. The number of events at each dot is
 429 represented by the diameter of the dot and the number of events. (a) Wire breaks. (b) Hammer blows.

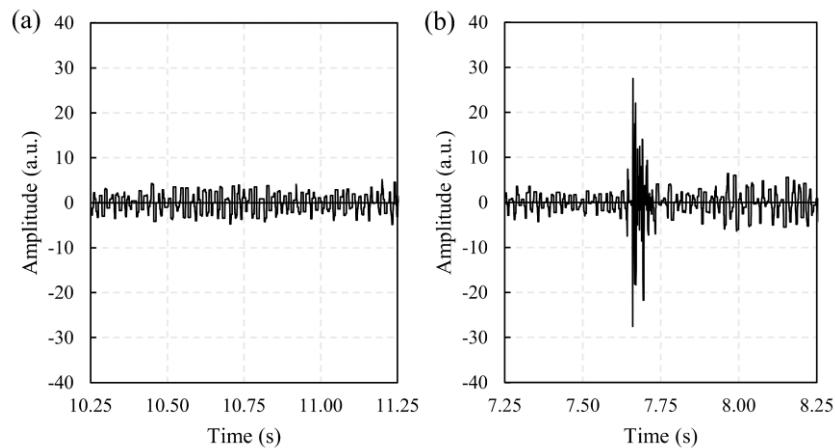
430 Regarding wire breaks, the section with the highest ZCRxSTE coincided with the segment
 431 where the signal originated in 70% of the detected events. Hence, the location accuracy was 10
 432 m (the system’s spatial resolution). In the remaining 30%, the location was obtained on a 20-
 433 meter segment, i.e., in 100% of these events, the wire break was found on the 10-meter segment
 434 adjacent to the segment with the highest ZCRxSTE (see Figure 11a).

435 Hammer blows were events that generated much higher vibrations than wire breaks. In their
 436 case, the coincidence between the 10-meter fibre segment with the highest ZCRxSTE and the
 437 segment where the signal originated was 48%. In the remaining 52%, in most of the events
 438 (87%), the location was obtained with an accuracy of 20 m, while in a low percentage (13%),
 439 the accuracy was 30 m, as observed in Figure 11b.

440 Consequently, it can be concluded that the DAS system used had an accuracy of 20 m in
 441 locating 100% of the wire breaks and almost 90% of the hammer blows. Although the system
 442 was not very accurate in detecting the fibre segment where the hammer blows originated, it
 443 showed high accuracy in detecting lower vibration signals such as wire breaks, which are the
 444 most interesting in this project for the early detection of structural failure of prestressed
 445 concrete pipes.

446 3.3.3. Presence of background noise

447 Continuous acoustic signals from devices or machines, such as the one generated by the power
 448 generator placed on the buried section of SP (see Figure 2), show a series of dominant
 449 frequencies while the device operates. This means the signal obtained after applying the
 450 denoising filters is still very noisy (see Figure 12a). Nevertheless, when an impulse-type event
 451 such as the ones analysed in this paper, which excites multiple frequencies, occurred, the DAS
 452 system showed a signal disturbance such as the one shown in the example in Figure 12b.



453

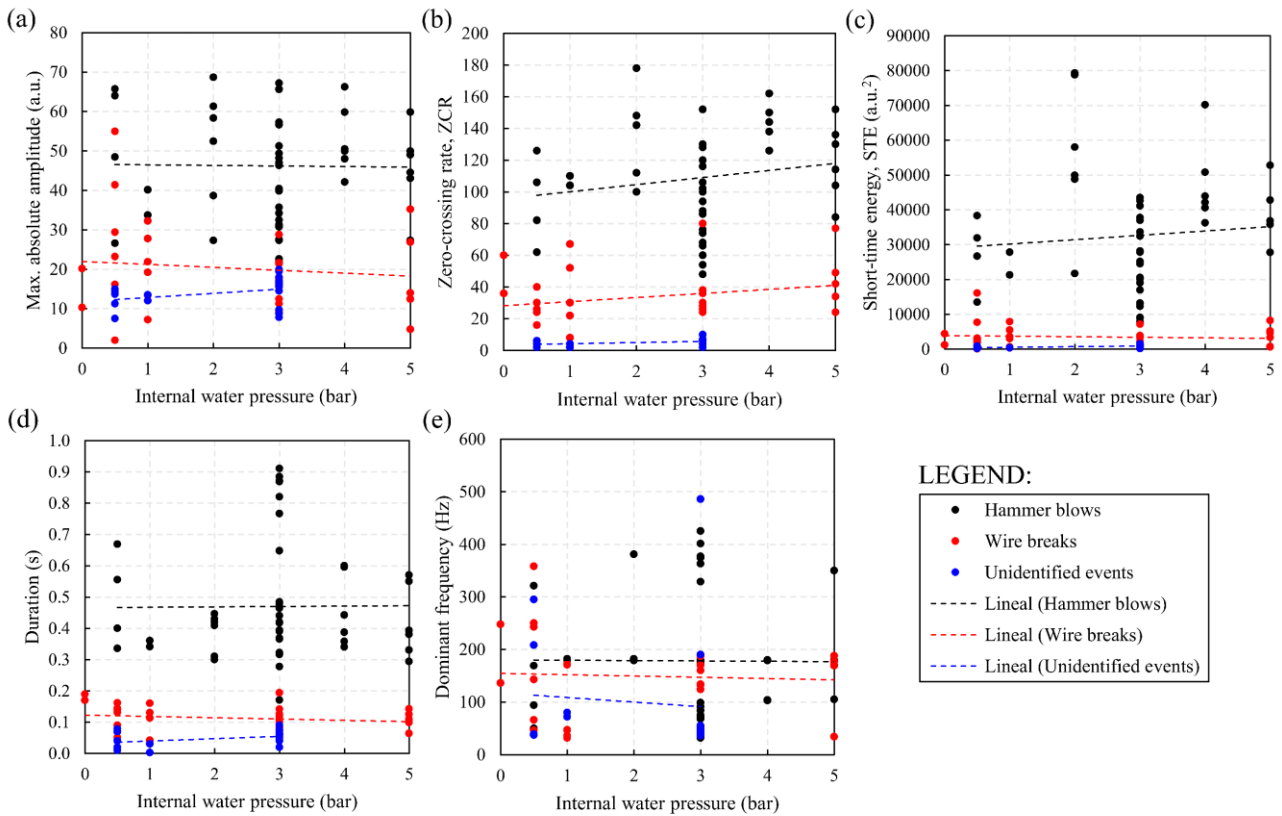
454 Figure 12: Example of the signal with background noise after applying the high-pass and denoising filters. (a)
 455 Only background noise. (b) Wire break with background noise.

456 The signal obtained from the events analysed when the power generator was running showed
 457 very similar values for all the parameters to those of the events without background noise. For
 458 this reason, all these events were included in the plots in Figure 9 and Figure 10a. Figure 10b
 459 represents again the relationship between ZCR and STE of Figure 10a but highlights the events
 460 with background noise. It shows the similarity of the parameters obtained for these signals with
 461 those of the signals without background noise, as they generally locate in the same areas
 462 represented in Figure 10a. It should be noted that on two occasions, the wire break signal was
 463 comparable to the unidentified event signal, either because those two wire breaks in particular
 464 produced low vibrations or because the background noise masked the wire break signal.

465 The analysis in this section demonstrates that the signals studied in this paper, from both wire
 466 breaks and hammer blows, could be identified by the DAS system used despite the existence
 467 of background noise from continuous acoustic signals from devices or machines. These events
 468 produced signals whose main measured parameters showed similar values to those of events
 469 without background noise, as shown in Figure 10b. This characteristic will facilitate their
 470 implementation in future signal detection algorithms.

471 3.3.4. Internal water pressure

472 Figure 13 shows the values of the different parameters analysed as a function of the internal
 473 water pressure in the pipeline. The three types of events (wire breaks, hammer blows and
 474 unidentified events) have been included in the graphs. Linear trend lines have also been plotted
 475 for each data set to observe better possible relationships between the parameters and the
 476 internal pressure.



477

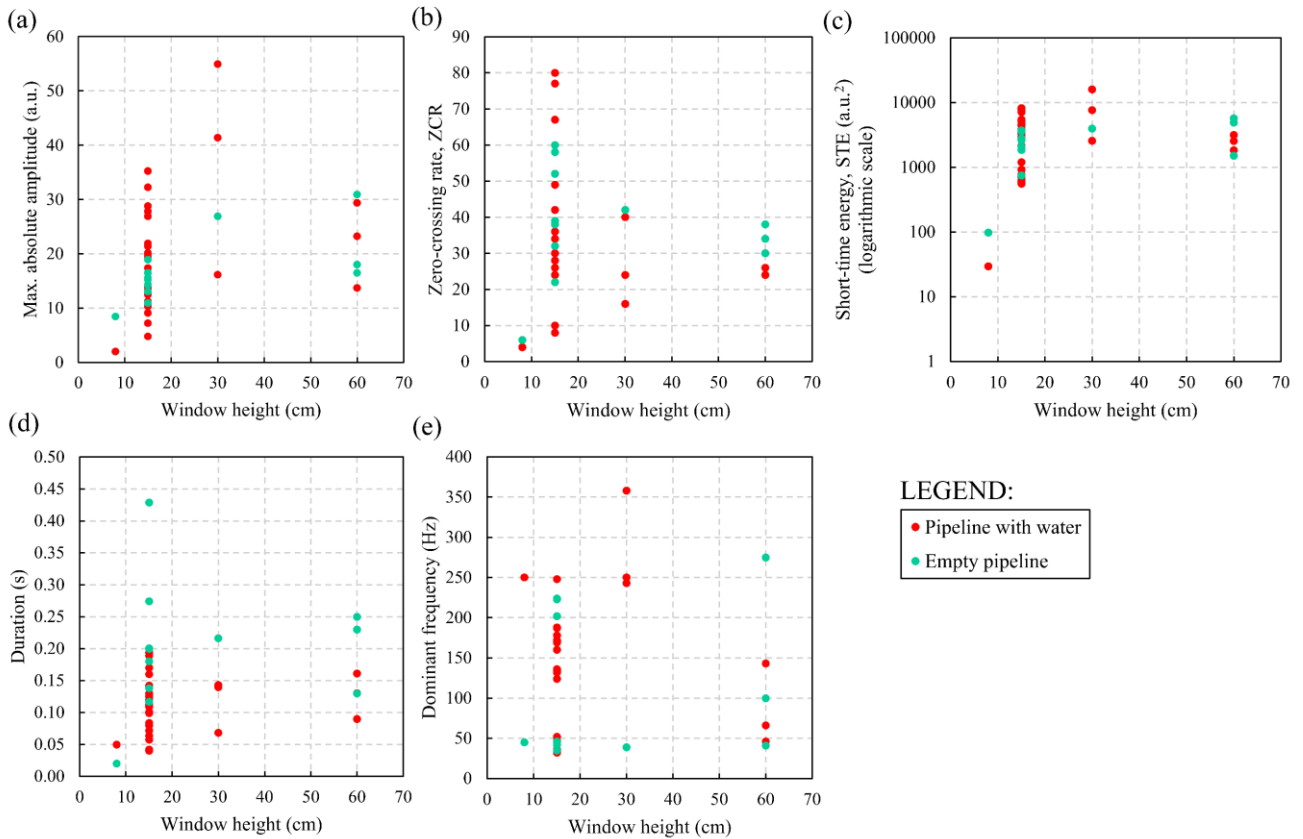
478 Figure 13: Relationship between the values of the parameters analysed for all events recorded in the pipeline
 479 with water and the internal water pressure. (a) Maximum absolute amplitude. (b) ZCR. (c) STE. (d) Duration.
 480 (e) Dominant frequency.

481 Figure 13 shows that, for the same value of internal pressure, events of the same type have a
 482 large dispersion for all parameters. Regarding the relationship of the parameters with the
 483 internal pressure, only the ZCR shows a certain upward trend so that the ZCR of the signal
 484 increases with the internal pressure, but, as already indicated, the dispersion of the results is so
 485 high that the linear fit can be considered erroneous (values of the determination coefficients
 486 below 0.2).

487 From the analysis carried out, it is concluded that the results obtained were not sufficient to
 488 show a clear relationship between the measured parameter and the internal water pressure in
 489 the pipeline. Consequently, the other variables considered in this experimental programme (see
 490 Section 2.1) have been analysed without differentiating the events according to the internal
 491 water pressure.

492 3.3.5. Size of the window in the mortar coating

493 The 46 shear cuts to simulate wire breaks were made in windows of different heights opened
 494 in the mortar to reveal the prestressed wire. As indicated above, the heights of these windows
 495 were 8, 15, 30 and 60 cm. The DAS system detected wire breaks in all cases except for three
 496 of the five wire breaks in the 8 cm high window. Figure 14 shows the relationship between the
 497 values of the parameters analysed for all the wire breaks recorded, both in the empty pipeline
 498 and the pipeline with water, and the window height.



499

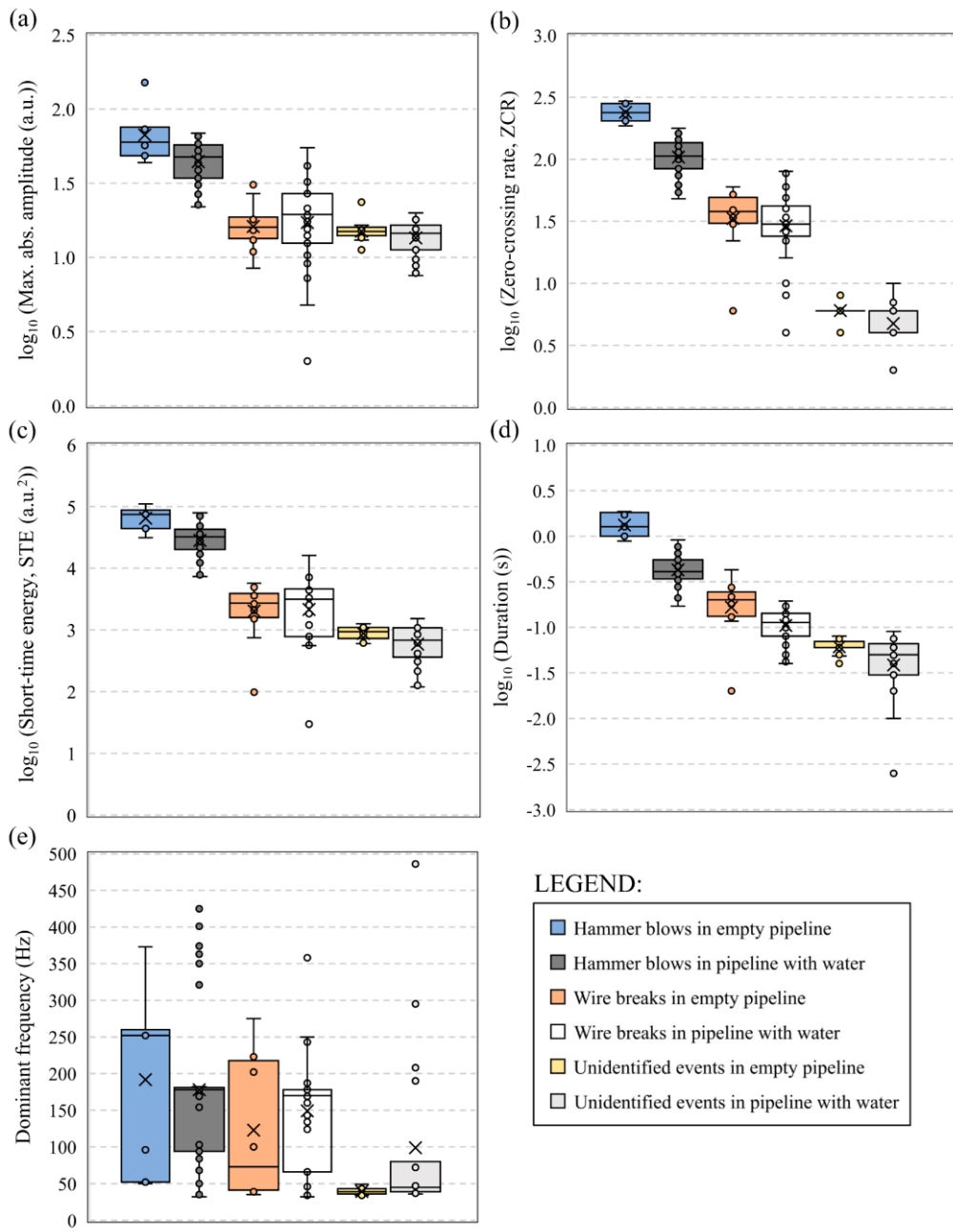
500 Figure 14: Relationship between the results of the parameters analysed for all wire breaks recorded and the
 501 window opening. (a) Maximum absolute amplitude. (b) ZCR. (c) STE. (d) Duration. (e) Dominant frequency.

502 The analysis of the parameters shows that the two wire breaks recorded in the 8 cm high
 503 window had very low values of the maximum absolute amplitude, the ZCR, the STE and the
 504 signal duration compared to those of the other windows. Note that in the STE, the large
 505 difference makes it necessary to use the logarithmic scale. In fact, in Figure 10a, these two wire
 506 breaks in the 8 cm high window are the two red dots that show the ZCR and STE values
 507 characteristic of the unidentified events area. However, there is no clear relationship between
 508 the parameter and the window height in the rest of the windows. On the other hand, again, the
 509 dominant frequency does not show any kind of trend between events with similar
 510 characteristics.

511 This analysis concluded that the DAS system can identify wire breaks when the uncovered
 512 wire length is around 15 cm or more. However, if the uncovered wire length is about 8 cm or
 513 less, the system may confuse the signal with that of a noise caused by an unidentified event or
 514 even fail to detect it. Consequently, if the corrosion of the wire is not limited to a particular
 515 area but extends more widely before reaching the wire break, the DAS system used will be able
 516 to identify wire breaks with a high probability. This kind of pathology, which causes spalling
 517 of the surrounding mortar and leaves a sufficient length of wire not subject to bonding with the
 518 concrete to vibrate freely after the wire break, was commonly observed in prestressed concrete
 519 pipes that failed under corrosion, such as those reported in ^{4,27,28}. Only in cases where the
 520 corrosion is very localised (local pitting corrosion), with very little or no spalling of the mortar,
 521 will the system have difficulties detecting a wire break since the high bond of the concrete to
 522 the wire prevents the release of high internal energy.

523 3.3.6. Presence of water in the pipeline

524 The tests performed on the empty pipeline were aimed at analysing the capacity to detect wire
 525 breaks using the DAS system when there is no water in the pipe, as Li et al. did in ¹⁵, since this
 526 situation can occur during the operation of water mains. Consequently, the parameters analysed
 527 for the three types of events (hammer blows, wire breaks and unidentified events) performed
 528 in the empty pipeline and the pipeline full of water were compared. Figure 15 shows this
 529 comparison using box-whisker plots. Note that the data from the pipeline with water were
 530 already presented in Figure 9, but are presented again together with the new data from the
 531 empty pipeline for ease of comparison.



532

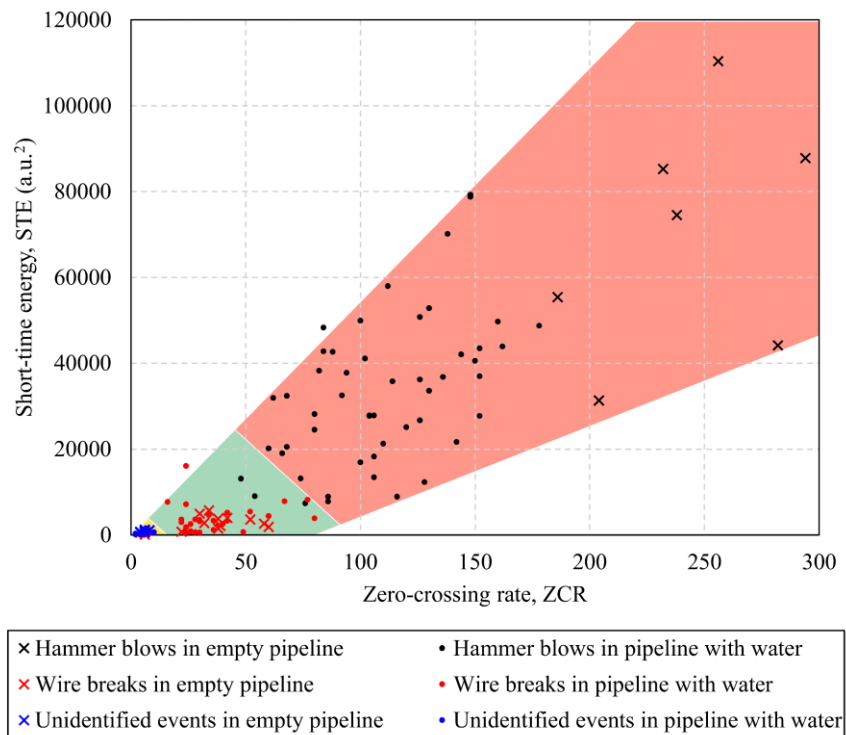
533 Figure 15: Box-whisker plots of the signals produced by hammer blows, wire breaks and unidentified events in
 534 the pipes with and without water for the five parameters analysed. (a) Maximum absolute amplitude. (b) ZCR.

535 (c) STE. (d) Duration. (e) Dominant frequency. (Note that the data presented in Figure 9 from the pipeline with
536 water are presented again in this figure for comparison with the data from the empty pipeline).

537 Figure 15a shows that, in terms of the maximum absolute amplitude, if we compare the hammer
538 blows in empty and full pipes, the boxes do not have an offset, but their values overlap, so that,
539 when detecting the events using this parameter, we would not be able to distinguish whether
540 the pipeline is full or empty. The same applies to wire breaks and unidentified events. In Figure
541 15b, the box boundaries of the hammer blows have a clear offset, so we can distinguish whether
542 the pipe is full or empty depending on the range in which the ZCR is located. However, this is
543 not observed for wire breaks and unidentified events, where again, the boundaries of the boxes
544 overlap. Figure 15c shows that it is not possible to distinguish whether the pipe is full or empty
545 based on the STE because the boxes overlap. However, Figure 15d, on the duration of the
546 signal, shows a clear difference between the full and empty pipeline, so that the events
547 performed in the empty pipeline present a signal of longer duration than those performed in the
548 pipeline full of water, for both hammer blows and wire breaks. This is not the case, however,
549 for the unidentified events, which show little difference in the duration of the signals when the
550 pipeline is full and empty. Finally, Figure 15e shows that, once again, the dominant frequency
551 is unrelated to the type of event or the presence or absence of water inside the pipe.

552 As a consequence of the above analysis, it is concluded that it is possible to differentiate
553 whether the pipeline is full or empty through the duration of the signals: the signals detected in
554 the empty pipeline showed a longer duration than in the pipeline full of water. This result makes
555 sense since water has a greater capacity than air to absorb the energy of the waves, i.e., to
556 dampen them, so the amplitude of the waves decreases more quickly than when the pipe is full
557 of air and, therefore, the signal dissipates more quickly.

558 On the other hand, it can be observed in Figure 15 that there are no significant differences in
559 ZCR and STE between the signals of empty and full pipes. Therefore, the possibility of using
560 these parameters to identify the type of event when the pipe is empty was studied, as in Section
561 3.3.1. Figure 16 represents all the events analysed in this paper, both with full and empty
562 pipelines, and it can be observed that the same differentiated areas in Figure 10 are still
563 observed, which allows for identifying the type of event detected in the water main. Note that
564 the boundaries of the area of hammer blows were prolonged to reach higher values of ZCR and
565 STE.



566

567
568

Figure 16: STE-ZCR plot of the signals produced by hammer blows, wire breaks and unidentified events in the pipes with and without water.

569 4. Conclusions

570 This paper presents the experimental work carried out to study the capability of an easy-to-
571 install DAS system using fibre optics to identify and locate the acoustic signal produced by
572 wire breaks in pre-stressed concrete drinking water pipes to perform early detection of possible
573 structural failures. The signals from wire breaks made in a large experimental pipeline built on
574 purpose for this research were analysed and differentiated from other sounds of similar
575 characteristics (hammer blows and noises coming from unidentified events). The most relevant
576 aspects to be highlighted from this research are presented in the following paragraphs.

577 Firstly, although the fibre optic cable was loose inside the pipe (for ease of installation) instead
578 of bonded to the pipe walls, the DAS system used was able to identify wire breaks in 93% of
579 the 46 cases studied. The undetected wire breaks corresponded to cases where the length of
580 prestressed wire not bonded to the concrete had the smallest dimension (8 cm). This case would
581 correspond in a real scenario to very localised wire corrosion with little or no spalling of the
582 mortar coating. Nonetheless, the corrosion failures reported in the literature showed high
583 degrees of spalling.

584 Secondly, the combination of the zero-crossing rate (ZCR) and short-time energy (STE) values
585 of the signals proved to be a good indicator of the cause of the detected event among the three
586 types of events analysed (wire breaks, hammer blows and unidentified events), whether the
587 events had occurred with the pipe full of water or empty, and whether there was background
588 noise from a power generator. The combination of the ZCR and STE results made it possible
589 to distinguish the signal's origin by means of three differentiated ranges of values.

590 Thirdly, the DAS system could detect with an accuracy of 20 m the location of 100% of the
591 detected wire breaks and almost 90% of the hammer blows by determining the fibre segment
592 where the highest ZCRxSTE occurs.

593 In addition, no relationship was observed between the analysed signal parameters (maximum
594 absolute amplitude, ZCR, STE, duration and dominant frequency) and the internal water
595 pressure.

596 Furthermore, the wire breaks detected when the length of wire not subject to bonding with the
597 concrete was 8 cm showed very low ZCR and STE values, which were comparable to those
598 obtained for noises coming from unidentified events. However, the wire breaks caused when
599 the free length of the wires was 15, 30 and 60 cm showed higher ZCR and STE values that
600 were very similar to each other.

601 Finally, the duration of the signals proved to be a good indicator of the existence or not of water
602 inside the pipeline so that the events produced when the pipe was empty presented, in general,
603 a longer duration than those produced when the pipe was full of water. However, the signals
604 did not show significant differences by comparing the ZCR and STE, which made it possible
605 to distinguish the signals produced by the three events analysed in the same way when the pipe
606 was full and when it was empty.

607 It is worth noting that the results obtained in this paper present a highly promising perspective
608 on the use of the easy-to-install DAS system used in this research for the early detection of
609 structural problems in prestressed concrete pipes. In the future, the research team will focus on
610 implementing the results in an algorithm for processing and identifying the signals obtained by
611 the DAS system for the long-term monitoring of a longer section of pipe in operation. Likewise,
612 it would be of great interest to study the capacity of the DAS system to detect other signals that
613 prematurely indicate the possible structural failure of concrete pipes due to other reasons, such
614 as crushing, to improve the algorithm for the premature detection of structural failure. This
615 work could be complemented using machine learning to create a Pattern Recognition System
616 (PRS). Further work may involve the development of a condition assessment programme to
617 determine when pipes should be replaced based on the level of damage they have exhibited
618 during continuous monitoring.

619 **Data Availability**

620 The data used to support the findings of this study are available from the corresponding author
621 upon request.

622 **Conflicts of Interest**

623 The authors declare that there is no conflict of interest regarding the publication of this paper.

624 **Funding Statement**

625 The Regional Government of Valencia (Spain), through the Valencian Innovation Agency
626 (AVI) and “ERDF A way of making Europe”, supported the present research work through the
627 grant [INNEST/2021/201].

628 **Acknowledgements**

629 The authors thank the support and collaboration in this research of CalSens S.L. and the
630 Concrete Science and Technology University Institute (ICITECH) of the Universitat
631 Politècnica de València (UPV; Spain).

632 **References**

- 633 1. Toreti A, Bavera D, Acosta Navarro J, et al. *Drought in Europe March 2023*.
634 Luxembourg. Epub ahead of print 2023. DOI: 10.2760/998985.
- 635 2. Higgins MS, Paulson PO. Fiber Optic Sensors for Acoustic Monitoring of PCCP.
636 *Pipelines 2006*.
- 637 3. Atherton DL, Morton K, Mergelas BJ. Detecting breaks in prestressing pipe wire. *J Am*
638 *Water Works Assoc* 2000; 92: 50–56.
- 639 4. Bell GEC, Paulson P, Galleger JJ, et al. Use of Acoustic Monitoring Data for PCCP
640 Condition Assessment. In: *Pipelines Specialty Conference 2009*. 2009.
- 641 5. Hajali M, McNealy A, Dettmer A. Scattered Broken Wire Wrap Effects on Structural
642 Capacity of Prestressed Concrete Cylinder Pipes. In: *Pipelines 2020*. Reston, VA:
643 American Society of Civil Engineers, 2020, pp. 111–122.
- 644 6. Loganathan K, Najafi M, Kaushal V, et al. Development of a Decision Support Tool for
645 Inspection and Monitoring of Large-Diameter Steel and Prestressed Concrete Cylinder
646 Water Pipes. *J Pipeline Syst Eng Pract*; 13. Epub ahead of print 2022. DOI:
647 10.1061/(ASCE)PS.1949-1204.0000603.
- 648 7. Huang J, Zhou Z, Zhang D, et al. Online monitoring of wire breaks in prestressed
649 concrete cylinder pipe utilising fibre Bragg grating sensors. *Measurement* 2016; 79:
650 112–118.
- 651 8. Travers FA. Acoustic monitoring of prestressed concrete pipe. *Constr Build Mater* 1997;
652 11: 175–187.
- 653 9. Lenghi A, Amaitik N, Wrigglesworth M. Expansion of Existing Monitoring System on
654 Great Man-Made River Project Using Acoustic Fibre Optic Technology. *Water Pract*
655 *Technol*; 3. Epub ahead of print 1 September 2008. DOI: 10.2166/wpt.2008.072.
- 656 10. Zhu H-H, Liu W, Wang T, et al. Distributed Acoustic Sensing for Monitoring Linear
657 Infrastructures: Current Status and Trends. *Sensors* 2022; 22: 7550.
- 658 11. Tanimola F, Hill D. Distributed fibre optic sensors for pipeline protection. *J Nat Gas Sci*
659 *Eng* 2009; 1: 134–143.
- 660 12. Wu H, Sun Z, Qian Y, et al. A hydrostatic leak test for water pipeline by using
661 distributed optical fiber vibration sensing system. In: Lee B, Lee S-B, Rao Y (eds). 2015,
662 p. 965543.

- 663 13. Stajanca P, Chruscicki S, Homann T, et al. Detection of Leak-Induced Pipeline
664 Vibrations Using Fiber—Optic Distributed Acoustic Sensing. *Sensors* 2018; 18: 2841.
- 665 14. Hussels M-T, Chruscicki S, Arndt D, et al. Localization of transient events threatening
666 pipeline integrity by fiber-optic distributed acoustic sensing. *Sensors (Switzerland)*; 19.
667 Epub ahead of print 2019. DOI: 10.3390/s19153322.
- 668 15. Li Y, Sun K, Si Z, et al. Monitoring and identification of wire breaks in prestressed
669 concrete cylinder pipe based on distributed fiber optic acoustic sensing. *J Civ Struct*
670 *Health Monit*. Epub ahead of print 9 August 2022. DOI: 10.1007/s13349-022-00605-0.
- 671 16. Ma B, Gao R, Zhang J, et al. A YOLOX-Based Automatic Monitoring Approach of
672 Broken Wires in Prestressed Concrete Cylinder Pipe Using Fiber-Optic Distributed
673 Acoustic Sensors. *Sensors* 2023; 23: 2090.
- 674 17. Tejedor J, Macias-Guarasa J, Martins HF, et al. A multi-position approach in a smart
675 fiber-optic surveillance system for pipeline integrity threat detection. *Electronics*
676 *(Switzerland)* 2021; 10: 1–19.
- 677 18. Wu H, Chen J, Liu X, et al. One-Dimensional CNN-Based Intelligent Recognition of
678 Vibrations in Pipeline Monitoring With DAS. *Journal of Lightwave Technology* 2019;
679 37: 4359–4366.
- 680 19. Bai Y, Xing J, Xie F, et al. Detection and identification of external intrusion signals
681 from 33 km optical fiber sensing system based on deep learning. *Optical Fiber*
682 *Technology* 2019; 53: 102060.
- 683 20. Zuo J, Zhang Y, Xu H, et al. Pipeline Leak Detection Technology Based on Distributed
684 Optical Fiber Acoustic Sensing System. *IEEE Access* 2020; 8: 30789–30796.
- 685 21. Bell GEC, Paulson P. Measurement and Analysis of PCCP Wire Breaks, Slips, and
686 Delaminations. In: *Pipelines 2010: Climbing New Peaks to Infrastructure Reliability:*
687 *Renew, Rehab, and Reinvest*. 2010.
- 688 22. Clark BL, Paulson PO, Bell GEC, et al. Advanced acoustic monitoring for PCCP. In:
689 *Pipelines 2014: From Underground to the Forefront of Innovation and Sustainability -*
690 *Proceedings of the Pipelines 2014 Conference*. 2014, pp. 256–266.
- 691 23. Higgins MS, Stroebele A, Zahidi S. Numbers don't lie, PCCP performance and
692 deterioration based on a statistical review of a decade of condition assessment data. In:
693 *Pipelines 2012: Innovations in Design, Construction, Operations, and Maintenance -*
694 *Doing More with Less - Proceedings of the Pipelines 2012 Conference*. 2012, pp. 298–
695 306.
- 696 24. CEN. UNE-EN ISO 6892-1:2017 Metallic materials - Tensile testing - Part 1: Method
697 of test at room temperature. 2017.
- 698 25. Pastor Graells J. *Chirped-Pulse Phase-Sensitive Optical Time Domain Reflectometry*.
699 University of Alcalá, 2018.

- 700 26. Fernandez-Ruiz MR, Pastor-Graells J, Martins HF, et al. Laser Phase-Noise
701 Cancellation in Chirped-Pulse Distributed Acoustic Sensors. *Journal of Lightwave*
702 *Technology* 2018; 36: 979–985.
- 703 27. Wrigglesworth M, Higgins MS. When to intervene? Using rates of failure to determine
704 the time to shut down your PCCP line. In: *Pipelines 2010: Climbing New Peaks to*
705 *Infrastructure Reliability - Renew, Rehab, and Reinvest - Proc. of the Pipelines 2010*
706 *Conference*. 2010, pp. 803–814.
- 707 28. Valiente A. Stress corrosion failure of large diameter pressure pipelines of prestressed
708 concrete. *Eng Fail Anal* 2001; 8: 245–261.
- 709